Current Chemistry Letters 14 (2025) 183–192

Contents lists available at GrowingScience

Current Chemistry Letters

homepage: www.GrowingScience.com

Regioselectivity study of 1,3-dipolar cycloaddition of 2-azido-N-(4-diazenylphenyl)acetamide with terminal alkyne through DFT analysis

Khadija Zaki[a*], Abdelouahid Sbai[a*], Mohammed Bouachrine[a] and Tahar Lakhlifi[a]

[a]*Molecular Chemistry and Natural Substances Laboratory, Moulay Ismail University, Faculty of Science, bp 11201 Meknes, Morocco*

C H R O N I C L E

Article history:
Received February 25, 2024
Received in revised form
March 25, 2024
Accepted July 3, 2024
Available online
July 3, 2024

Keywords:
Click reaction
1,3-dipolar cycloadditions
1,2,3-triazole
Regioselectivity
DFT calculations

A B S T R A C T

The mechanism and regioselectivity of 1,3-dipolar reaction of 2-azido-N-(4-diazenylphenyl) acetamide and an alkyne have been studied in gas phase and in DMSO using the B3LYP-GD3 functional and 6-31G(d,p) basis set. The reaction followed a one-step mechanism with asynchronous TSs. The calculated global reactivity indices calculated revealed, among other things, the nucleophile character of the 2-azido-N-(4-diazenylphenyl)acetamide and the electrophile character of the alkyne (4-bromo-2-chloro-1-ethynylbenzene), in addition to an electron transfer from the 4-bromo-2-chloro-1-ethynylbenzene towards the 2-azido-N-(4-diazenylphenyl) acetamide. The calculated local reactivity indices predicted the formation of the 1,4-triazole, with the most nucleophilic nitrogen and the most electrophilic carbon favoring its formation. However, analysis of the activation energies and thermochemistry parameters showed that the 1,5 triazole is energetically favorable and more stable under thermodynamic control. Bond order analysis coupled with bond formation evolution and the solvent effect was further investigated to support and highlight the asynchronicity in bond formation and the regioselectivity of the reaction, respectively.

1. Introduction

Triazoles, a class of five-membered heterocyclic compounds containing three nitrogen atoms and two sp² carbon atoms, have garnered significant attention due to their diverse biological activities and wide range of applications in pharmaceuticals, agriculture, and materials science. These compounds are known for their stability, ability to form strong hydrogen bonds, and resistance to metabolic degradation, making them valuable in drug design and development. The synthesis of triazoles dates back to 1963, when Rolf Huisgen first described their formation via the reaction of an alkyne with an azide,[1] a process known as 1,3-dipolar cycloaddition. This seminal work laid the foundation for further exploration of triazole chemistry and introduced the concept of 1,3-dipolar cycloaddition reactions, where a 2-azido-N-(4-diazenylphenyl) acetamide (such as an azide) reacts with a 4-bromo-2-chloro-1-ethynylbenzene (such as an alkyne) to form a five-membered ring.

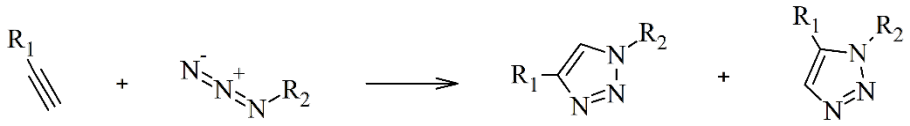

Traditional 1,3-dipolar cycloadditions are generally non-regioselective, yielding a mixture of 1,4- and 1,5-triazole isomers. The lack of regioselectivity in these thermal cycloadditions poses a challenge for the efficient synthesis of specific triazole derivatives, which is crucial for their application in targeted drug development. However, significant advancements have been made to improve the regioselectivity of these reactions. One notable breakthrough came in 2002 when Sharpless

* Corresponding author
E-mail address kha.zaki@edu.umi.ac.ma (K. Zaki) a.sbai@umi.ac.ma (S. Sbai)

doi: 10.5267/j.ccl.2024.7.001

and coworkers introduced a copper-catalyzed version of the reaction, which specifically produced the 1,4-triazole isomer.[2–5] This copper-catalyzed reaction, classified as a "click reaction" due to its simplicity, reliability, and high regioselectivity, has become a cornerstone of triazole synthesis. Click chemistry, with its mild reaction conditions and high yields, has revolutionized the synthesis of complex molecules, allowing for the rapid assembly of libraries of biologically active compounds.

Regioselectivity in triazole formation can be further enhanced through two main strategies: (i) the use of transition metal (TM)-type catalysts[6] and (ii) the incorporation of electron-withdrawing group (EWG)-activated alkenes or alkynes.[7] Transition metal catalysts, particularly those based on copper, palladium, and ruthenium, have been shown to lower the activation energy and direct the formation of specific triazole isomers. These catalysts can stabilize intermediates and transition states, providing a pathway for the selective formation of 1,4- or 1,5-triazole adducts. Alternatively, EWG-activated substrates can influence the electronic properties of the reacting species, thereby favoring the formation of the desired regioisomer. The presence of electron-withdrawing groups can enhance the electrophilicity of the alkyne, leading to a more controlled and regioselective cycloaddition process.

Understanding the mechanisms of 1,3-dipolar cycloaddition (32CA) reactions is crucial for rational design and optimization. These mechanisms can be broadly classified into non-polar and polar pathways. Non-polar mechanisms include synchronous concerted processes and stepwise biradical mechanisms, where intermediates such as diradicals may form during the reaction. In synchronous concerted mechanisms, the bonds are formed simultaneously in a single transition state, whereas in stepwise biradical mechanisms, the reaction proceeds through a diradical intermediate. Polar mechanisms, on the other hand, encompass one-step,[7–9] two-stage processes and stepwise zwitterionic pathways,[10–12] where the reaction proceeds through charged intermediates. In one-step, two-stage mechanisms, the reaction involves an initial charge-separated intermediate that subsequently rearranges to form the product, while in stepwise zwitterionic mechanisms, the reaction proceeds through a sequence of charged intermediates.

Non-polar mechanisms often involve a single transition state leading to product formation, while polar mechanisms can exhibit a more complex energy landscape with multiple intermediates and transition states. Density functional theory (DFT) and other computational methods have been instrumental in elucidating these pathways, providing insights into the energy profiles and key transition states involved. Computational studies enable the prediction of reaction outcomes and the identification of factors that influence regioselectivity, such as electronic and steric effects.

In this research, we conduct a comprehensive DFT-based study of the energy profile and mechanisms of 1,3-dipolar cycloaddition reactions, specifically focusing on the formation of triazole adducts from 2-azido-N-(4-diazenylphenyl)acetamide and terminal alkynes. The adduct of this reaction was obtained through a lead optimization of antimicrobial agents, [13,14] by substituting a fragment on the lead compound followed by a biological evaluation. By studying these reaction avenues concerning the modification appointed to the lead compound and how it affects the electronic behavior and energy profile of the reaction can help researchers by giving them an energetic view of the reaction for further optimization, in addition to offering ideas on the biological activity and its relation with energies, if there is any. By applying frontal orbital theory, stationary point theory, transition state theory, and global and local DFT-derived indices, we aim to deepen our understanding of the factors influencing regioselectivity and the underlying reaction mechanisms. This study provides valuable insights into the design of regioselective cycloadditions and the development of new triazole-based compounds with potential applications in various fields, including medicinal chemistry and materials science.

2. Results and Discussion

2.1 Reactivity analysis of reactants: Conceptual DFT Indices analysis at ground state reactants

2.1.1 Global reactivity indices

In order to understand the behavior of each reactant in this 1,3-dipolar reaction, global indices of reactivity were calculated using Eqs. (1-8) and the results are reported in **Table 1**.

Table 1. Electronic chemical potential (μ), chemical hardness (η), global electrophilicity (ω), global nucleophilicity (N), and global softness (S), the electronegativity (χ) of both 1.3-dipole and 4-bromo-2-chloro-1-ethynylbenzene in the gas phase. All values in eV units are calculated at B3LYP, GD3/6- 31G(d,p) level of theory

	E_{Homo}	E_{Lumo}	η	S	μ	χ	ω	N
2-azido-N-(4-diazenylphenyl) acetamide	-6.32	-1.94	2.19	0.46	-4.13	4.13	18.67	3.05
4-bromo-2-chloro-1-ethynylbenzene	-6.53	-1.41	2.56	0.39	-3.97	3.97	20.16	2.84

As the table shows, the nucleophilicity of the 2-azido-N-(4-diazenylphenyl) acetamide is higher than that of the 4-bromo-2-chloro-1-ethynylbenzene (3.05 eV > 2.84 eV), which means in this reaction, the dipole has a nucleophilic character, thus, it is the molecule that will contribute by its electrons of the Highest Occupied Molecular Orbital. Similarly, the 4-bromo-2-chloro-1-ethynylbenzene has the highest value of electrophilicity index, therefore it has an electrophile behavior and will contribute by its Lowest Unoccupied Molecular Orbital.

Looking at the chemical potential, we can determine which system is likely to lose or gain particles. High values indicate that it is prone to lose particles and vise-versa. In this case study, the chemical potential of the 4-bromo-2-chloro-1-ethynylbenzene is higher than that of the 2-azido-N-(4-diazenylphenyl) acetamide, which designates an electron transfer from the 4-bromo-2-chloro-1-ethynylbenzene towards the dipole. As for the hardness, it is the measure of the resistance of a molecule to undergo a chemical reaction, high values indicate the low reactivity of the molecule, while low values indicate its high reactivity and less stability. Compared to the 4-bromo-2-chloro-1-ethynylbenzene, the hardness of the dipole is lower (2.19 eV < 2.56 eV). In the table, the hardness and softness are reported side-by-side, for their inverse relationship with one another. While high values of hardness describe low reactivity and stability, high values of softness express high reactivity of molecules.

2.1.2 Local reactivity indices

The reaction originally generates two isomeric products, in which one is always favored. To profoundly understand the reactivity of each site in the reactants and therefore have an insight into the regioselectivity of the reaction, local reactivity

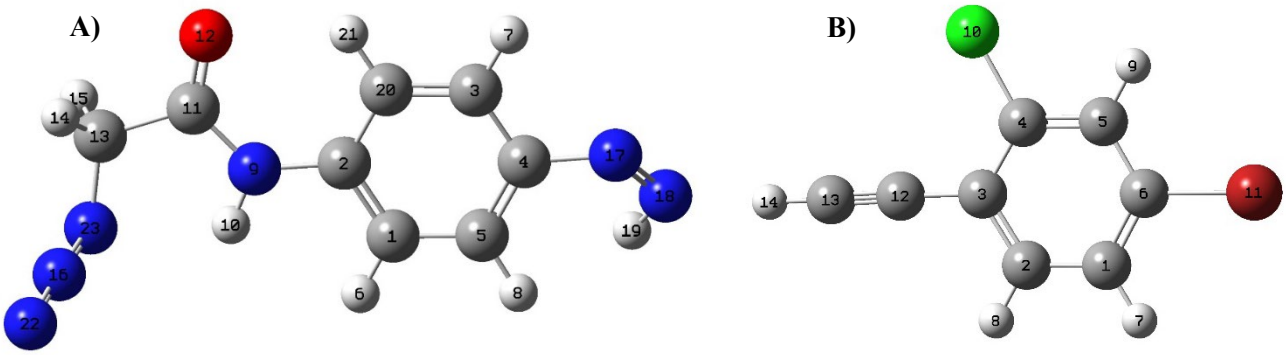

Fig. 1. Optimized reactants: 2-azido-N-(4-diazenylphenyl) acetamide (A) and 4-bromo-2-chloro-1-ethynylbenzene (B). indices were calculated using equations (9-12). The results are reported in Table 2.

Table 2. parr functions and local reactivity indices

	P+	P-	Wk	Nk
2-azido-N-(4-diazenylphenyl) acetamide				
N16	0.08	-0.01	1.50	-0.02
N22	0.17	0.02	3.23	0.05
N23	-0.02	0.03	-0.29	0.09
4-bromo-2-chloro-1-ethynylbenzene				
C12	-0.08	-0.06	-1.53	-0.16
C13	0.29	0.33	5.88	0.95

As previously explained, local reactivity indices highlight the reactive regions in the molecule, by providing an idea of the electrophilic and nucleophilic profile of each atom. Based on global reactivity indices, the 2-azido-N-(4-diazenylphenyl) acetamide has a nucleophilic character, and the 4-bromo-2-chloro-1-ethynylbenzene has an electrophilic character. This means we will be comparing nucleophilicity in dipole nitrogen atoms and electrophilicity for 4-bromo-2-chloro-1-ethynylbenzene carbon atoms. Figure 1 displays the optimized structure of both reagents, it is noteworthy that the numbering system is software generated, and displayed for distinguishing purposes only. The atoms involved in the cycloaddition reaction are N22, N23 in the 2-azido-N-(4-diazenylphenyl) , and C12, C13 in the 4-bromo-2-chloro-1-ethynylbenzene. The high local nucleophilicity indices of N23 define it as the most nucleophilic nitrogen, correspondingly C13 in the 4-bromo-2-chloro-1-ethynylbenzene reactant has the highest indices which identified it as the most electrophilic carbon.

According to Domingo's proposition in 2002, the interaction between two reactants in a cycloaddition reaction takes place between the most nucleophilic site in one and the most electrophilic site in the other.[15] The reported results which respect this conception favor the production of the 1,4 triazole isomer.

2.2 Transition states energy profile

A transition state search was performed to understand the mechanism of the proposed reaction and to have an energetic profile of the reaction. Activation and transition state energies are reported in Table 3.

Table 3. Transition state and activation energies in the presence and absence of the solvent

	Gas phase		In DMSO	
	E_{TS} (eV)	E_a (kcal/mol)	E_{TS} (eV)	Ea (kcal/mol)
1,4 triazole	-110271.4	21.2	-110272.0	20.4
1,5 triazole	-110271.9	9.5	-110272.3	12.1

Transition state and activation energies revealed the electronic stability and favoring of the 1,5 adduct, which disagrees with the previous findings of local reactivity indices. In the absence of the solvent, the activation energy barriers were in the order of 21.232 kCal/mol and 9.478 kcal/mol for 1,4 triazoles and 1,5 triazoles respectively. Similarly, in the presence of DMSO as a solvent, they were in the order of 20.442 kCal/mol and 12.069 kCal/mol for 1,4 and 1,5 triazoles respectively. Activation energies had slightly decreased for the 1,4 isomer, in the transition from the non-solvated state to the solvated state, while they increased for the 1,5 isomer.

2.3 Thermochemistry parameters analysis

Thermochemistry calculations are essential for predicting thermodynamic feasibility, energetics, and mechanism of cycloaddition reactions.

Table 4. Thermochemistry energies of the transition states and products, enthalpy, Gibbs free energy and entropy.

	Without solvent				DMSO			
	ΔH (kcal/mol)	ΔG (kcal/mol)	ΔE (kcal/mol)	ΔS (cal/mol.K)	ΔH (kcal/mol)	ΔG (kcal/mol)	ΔE (kcal/mol)	ΔS (cal/mol.K)
TS (1,4)	21.3	33.5	21.9	-40.8	20.7	33.4	21.3	-42.5
TS (1,5)	9.9	24.1	10.5	-47.7	12.4	26.3	13.0	-46.5
1,4 Triazole	-65.0	-49.8	-64.4	-50.8	-66.1	-115.9	-66.7	-80345.7
1,5 Triazole	-70.7	-55.0	-70.1	-52.7	-70.1	-119.9	-70.7	-84371.1

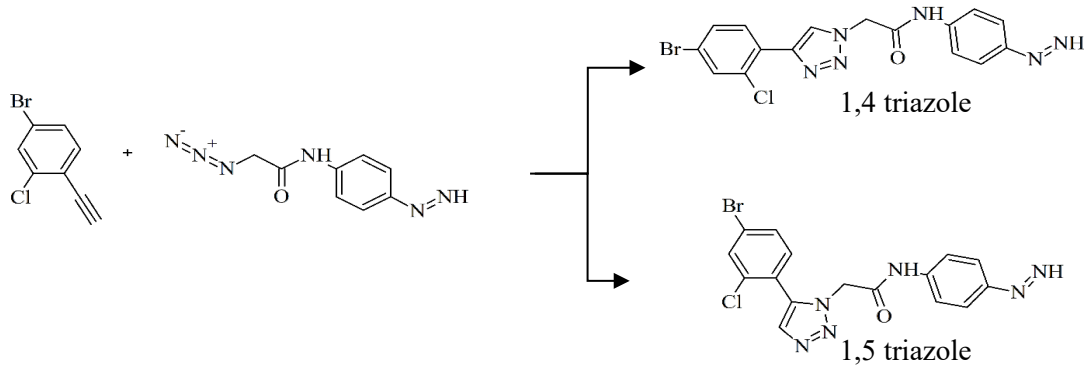

Fig. 2. Studied reaction paths for Triazole formation.

For the reaction of 2-azido-N-(4-diazenylphenyl)acetamide with terminal alkyne cycloaddition, following two different pathways, two possible products can be generated: The 1,4 and 1,5 triazoles. Stationary point determination permitted the localization of transition states TS1,4 and TS1,5, as well as the reactants and products at energy minima. The relative energy and thermochemistry data are grouped in Table 4. The analysis of the energy profiles suggests stability and favors the 1,5 triazole formation. The Gibbs free energy of the transition state relative to the formation of the 1,5 triazole is lower than that of the 1,4 triazole by 9.4 kcal/mol, as it is in the order of 33.5 kcal/mol in the 1,4 triazole transition state and in the order of 24.1 kcal/mol for the transition state of the 1,5 triazole adduct. Looking at the final formation of the product, the 1,5 triazole is the most stable product under thermodynamic control for it has the lowest Gibbs free energy in the order of -55.0 kcal/mol. The negative sign of the free energy designates the spontaneity of the reaction, and therefore it's an indication that it will proceed in the forward direction. The difference in the free energy of the two adducts is not large, in the order of 5.1kcal/mol, which indicates the formation of both products, non-selectively. These results support the activation energy values previously reported. The negative enthalpy values denote the exothermic character of the reaction. In DMSO solvent, the Gibbs free energy is nearly three times lower compared to the un-solvated state, which designates favoritism for the forward direction progress of the reaction. Furthermore, the 1,4 and 1,5 triazoles are more stable in DMSO than in gas phase, of course the 1,5 triazole has the lowest energy, but compared to the un-solvated state, the difference of Gibbs free energy values between the 1,4 and 1,5 triazole is only 5.0 kcal/mol. In terms of the remaining thermodynamic variables, 1,4 triazole is becoming increasingly favorable. Although it was not clearly observed, working in the presence of a solvent exhibited some degree of regioselectivity toward the 1,4 triazole. These results are in agreement with those of activation energy previously reported.

Table 5. TS bond length in A°

	TS 1,4 triazole gas phase	DMSO		TS 1,5 triazole gas phase	DMSO
N16-N17	1.268	1.262	**N16-N17**	1.265	1.263
N17-N18	1.162	1.164	**N17-N18**	1.172	1.173
C36-C35	1.238	1.240	**C36-C35**	1.241	1.241
N16-C36	2.137	2.109	**N16-C35**	2.255	2.258
N18-C35	2.292	2.314	**N18-C36**	2.117	2.123

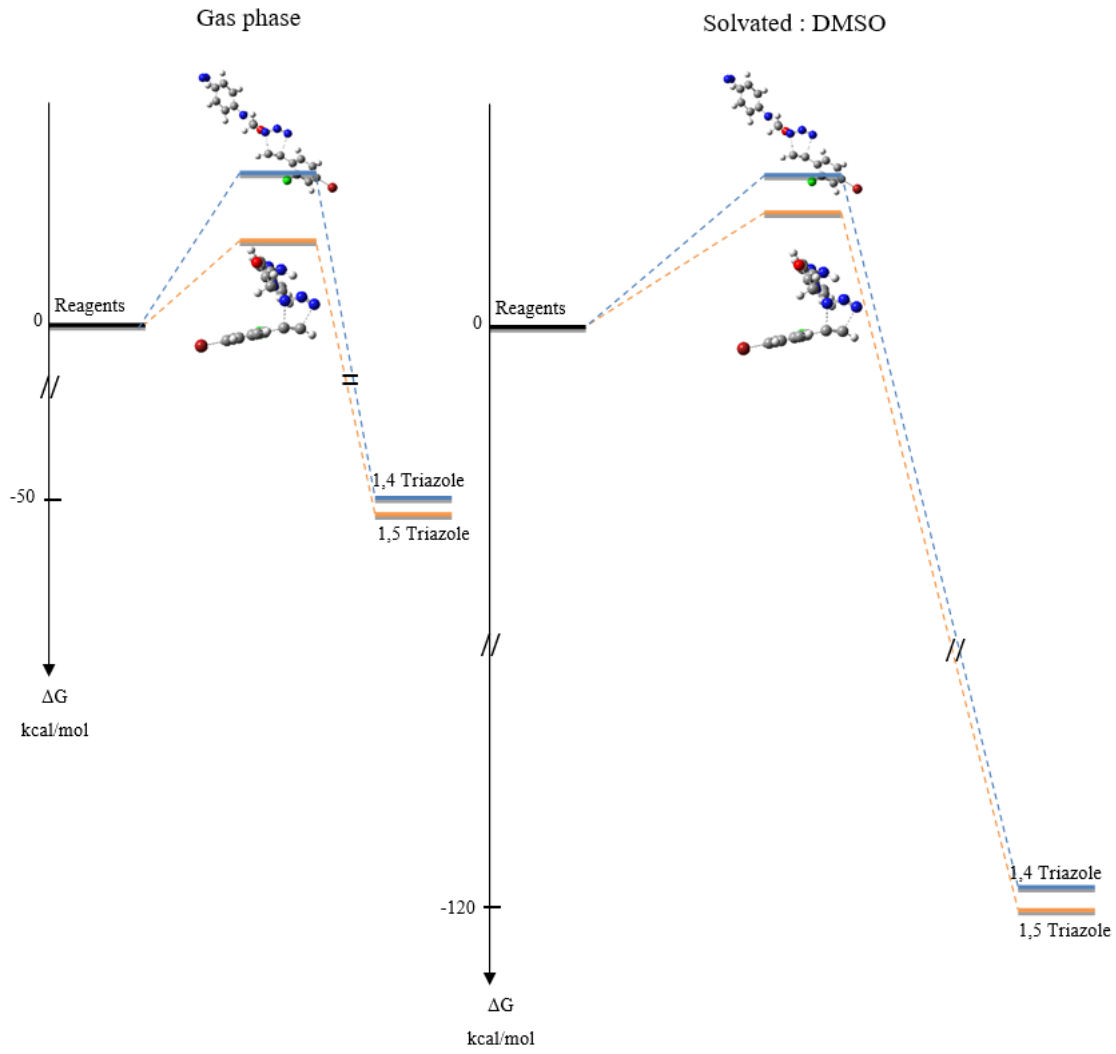

Fig. 3. Gibbs free energy profles (ΔG, in kcal/mol) in the gas phase and in the solvent at 1 atm and 289.15 K for the transition states and products of the reaction between 2-azido-N-(4-diazenylphenyl) acetamide and 4-bromo-2-chloro-1-ethynylbenzene.

Table 6 regroups bond lengths of broken and formed bonds. Bonds N16-C36 and N18-C35 are the two new formed bonds in the 1,4 triazole. As for 1,5 triazole it is the N16-C35 and N18-C36 new formed bonds. For the first isomer (1,4 triazole) the four reactive centers are distant from each other by 1.137 A° and 2.292 A° (gas phase), and 2.109 A° and 2.314 A° (in presence of DMSO). Whereas for the second isomer (1,5 triazole), bond distances were in the order of 2.255 A° and 2.117 A° (gas phase), and 2.258 A° and 2.123 A° (in DMSO solvent).

The observed parameters suggest that the transition states in question exhibit low levels of asynchronicity. This latter can be visualized by calculating the synchronicity extent [16] (Δd) between the new formed bonds for each isomer, for $TS_{1,4}$ it was in the order of 0.155 A° (0.205 A° in DMSO), whereas for $TS_{1,5}$ it was in the order of 0.138 A° (0.136 A° in DMSO).The longest TS bond length was registered for the N18-C35 bond in the 1,4 triazole in gas phase. Moreover, all these bond length values are within 2.117-2.292 A° range, and considering that the real Nitrogen-Carbon bond is in the order of 1.35-1.38 A° (view product bond length table), which is in agreement with literature values [17], we can safely say (we may deduce that) that the found TS bond length are not yet formed. (TS bond length is 1.5 times real bond length, which allow us to deduce that the observed TS bonds are not yet formed.)

Table 6. Bond lengths of the optimized Products in Å

	Product 1,4 triazole			Product 1,5 triazole	
	gas phase	DMSO		gas phase	DMSO
N16-N17	1.360	1.354	**N27-N28**	1.356	1.354
N17-N18	1.295	1.301	**N28-N29**	1.305	1.309
C36-C35	1.385	1.386	**C12-C13**	1.384	1.384
N16-C36	1.354	1.351	**N27-C12**	1.364	1.363
N18-C35	1.377	1.375	**N29-C13**	1.358	1.358

Transition states:

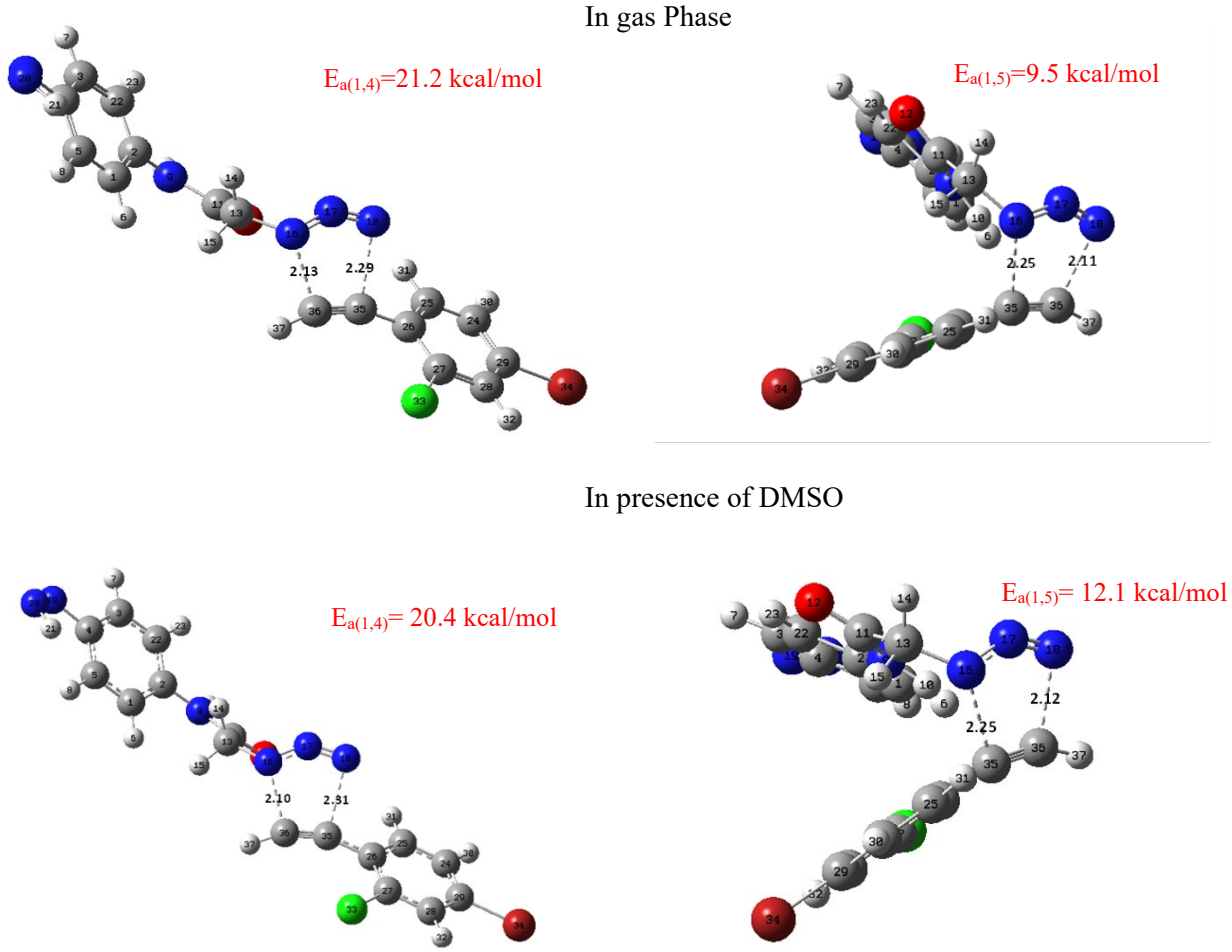

Fig. 4. B3LYP-D3/6-31G(d) optimized gas phase and in solvent geometries of the TSs. The distances in the forming-bond process are given in Å and the reported activation energies in kCal/mol (The numbering system is software generated, and displayed for distinguishing purposes only.)

2.4 Bond order analysis

Table 7 regroups the results of bond order analysis of the Transition states analyzed using Wiberg bond indices. [18,19]. The results indicate that the formation of the N-CH bond occurs before (is formed prior to) the N-C(R) bond. The evolution percentage of each of these bonds (i.e. N16-C36 and N18-C35) in $TS_{1.4}$ is in the order of 23.722% and 19.991% respectively. Similarly for the $TS_{1.5}$, N-C(H) bond order is a bit higher than that of N-C(R) with bond formation progress of 24.702% and 19.957%. The minimal discrepancy observed in the results supports our previous assumption of the low asynchronicity of bond formation.

Table 7. Bond order and formation progress

bond formation progress							
Gas phase							
1,4 triazole				**1,5 triazole**			
N16-C36		**N18-C35**		**N16-C35**		**N18-C36**	
TS	Product	TS	Product	TS	Product	TS	Product
0.290	1.224	0.258	1.293	0.241	1.208	0.339	1.374
23.722		19.991		19.957		24.702	
IN DMSO							
1,4 triazole				**1,5 triazole**			
N16-C36		**N18-C35**		**N16-C35**		**N18-C36**	
TS	Product	TS	Product	TS	Product	TS	Product
0.304	1.227	0.253	1.301	0.238	1.207	0.337	1.375
24.770		19.462		19.730		24.536	

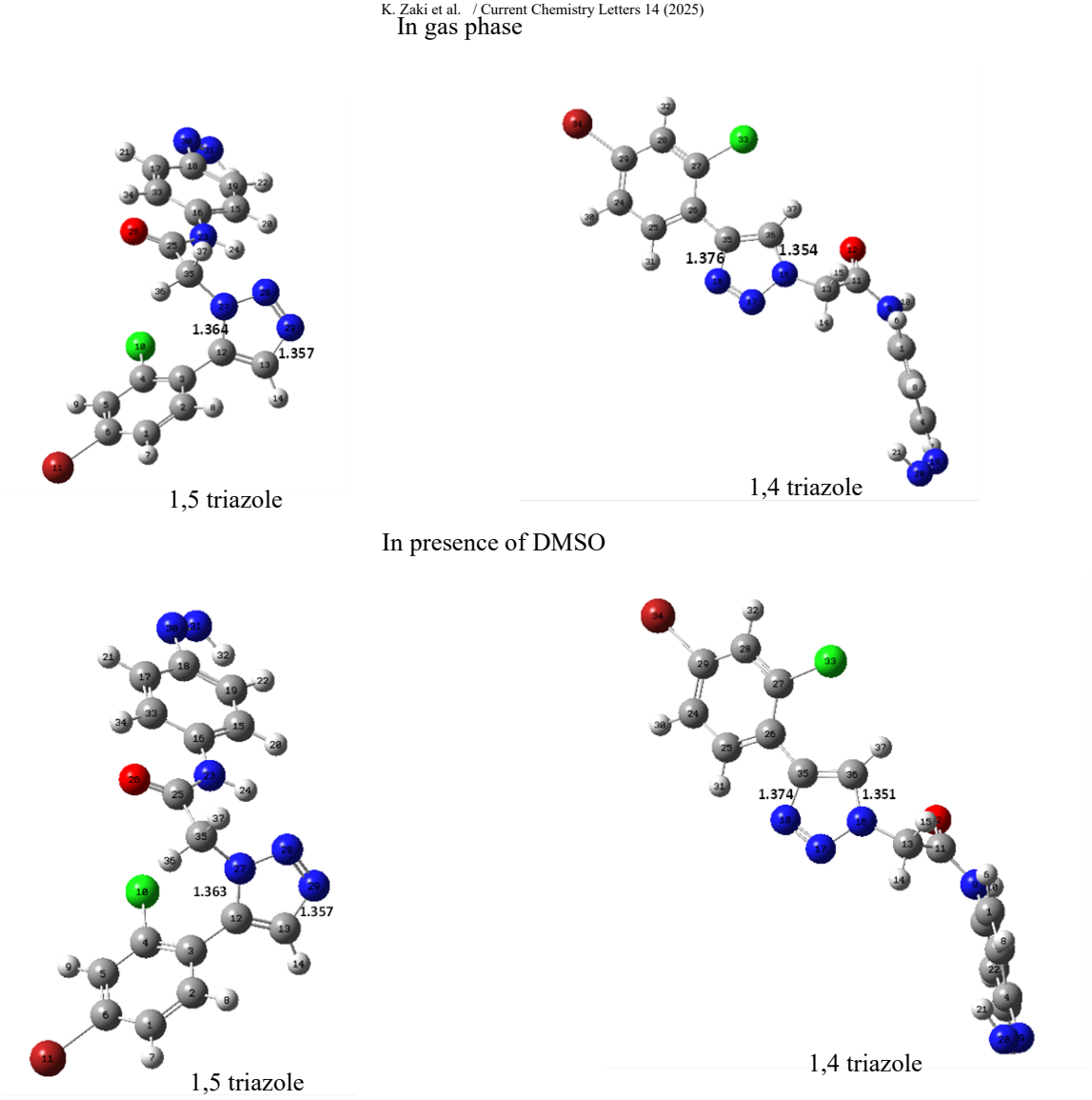

Fig. 5. B3LYP-D3/6-31G(d) optimized gas phase and in solvent geometries of the 1,5 and 1,4 triazoles. (The numbering system is software generated, and displayed for distinguishing purposes only.)

2.5 Frequency analysis of transition state optimized structures

The presence of an imaginary frequency confirms the correspondence of the found geometry to the saddle point on potential energy surface, and the associated normal mode represents a collective motion of the atoms in the molecule that leads to a change in the reaction coordinate. The $TS_{1,4}$ is confirmed with a 413.8996i cm^{-1} as an imaginary frequency that is coupled with a force constant of 1.0309 (mDyne/A), similarly the $TS_{1,5}$ is confirmed by 431.5906i cm^{-1} and 1.0368 mDyne/A, whereas each transition frequency is characterized with a unique eigenvalue. The observed low frequencies indicate the instability, and uphill in energy on the reaction pathway, which is extremely normal because transition states are geometries representing a highly energetic intermediate stage, where the bonds between the reactive molecules are in the process of forming or broking to form the product. Additionally, these values indicate that the bond between the nitrogen and carbon atoms in the transition state is moderately strong and has a moderate level of stiffness. The obtained TS frequency results are in the same range as other 1,3-dipolar reaction adducts, unlike those of other cycloaddition (e.g. Diels-Alder reaction), this difference can be attributed to the symmetrical charge distribution in Diels alder's reactions and the presence of a dipole in 1,3-dipolar reactions. Of course the nature of substituents in each reactive can play also a role in the stabilization of transition state and therefore its imaginary frequency.

3. Conclusions

The mechanism and regioselectivity of the 1,3-dipolar cycloaddition reaction of 2-azido-N-(4-diazenylphenyl)acetamide with terminal alkyne has been elucidated using DFT/B3LYP-D3/6-31G(d,p) level.

The analysis of DFT derived indices showed that the 2-azido-N-(substituted)acetamide indulges in the reaction by sharing its HOMO, and the terminal alkyne by its LUMO. The nucleophile comported molecule (i.e. 2-azido-N-(substituted)acetamide) was confirmed by an electron transfer towards the azide. Based on the local DFT derived indices, the favored product to form is the 1,4-triazole, for it includes the interaction between the most nucleophilic and electrophilic atoms in the 2-azido-N-(4-diazenylphenyl) acetamide and 4-bromo-2-chloro-1-ethynylbenzene respectively. Further calculation of activation energy and thermochemistry parameters however, identified the 1,5-triazole as the most favored adduct energetically under thermodynamic control, thus stable. Bond order and synchronicity extent revealed the asynchronous bond formation. In present of DMSO solvent, the reaction had tendency towards the 1,4-triazole, however, that regioselectivity is not enough to observe an energetic favoring.

4. Experimental

4.1. Materials and Methods

Density functional theory has proven its efficacy in transcribing the electronic behavior of molecules on several occasions, cycloaddition reactions being one of them.[20] The optimization of reactants, products, transition states, and the calculation of the various DFT-derived parameters [21] were all generated using the DFT method, B3LYB [22,23] as a functional, and 6-31G (d,p) [24] as basis set. To make sure that van der walls interactions are covered GD3 dispersion correction was added to the functional B3LYB.[25] Two types of descriptors were calculated, global and local reactivity indices. The first designates the overall reactivity of molecules, their indices provide insight into molecules' response to external stimuli and their potential for chemical reactions. In the present study, the calculated global reactivity indices are the following: Chemical potential, Global hardness, Global softness, electrophilicity, and nucleophilicity indices.

Electronegativity [26]

$$\chi = \frac{1}{2}(E_I + E_A) \tag{1}$$

where E_I and E_A ionization energy and electronic affinity respectively, and they are defined as:

$$E_I = E(N_0 - 1) - E(N_0) \tag{2}$$

$$E_A = E(N_0) - E(N_0 + 1) \tag{3}$$

Chemical potential[21]

$$\mu = \frac{E_{HOMO} + E_{LUMO}}{2} \tag{4}$$

Hardness[21]

$$\eta = \frac{1}{E_I - E_A} \tag{5}$$

Softness[21]

$$S = \frac{1}{\eta} = (E_I - E_A) \tag{6}$$

Electrophilicity [21,27,28]

$$\omega = \frac{\mu^2}{2\eta} \tag{7}$$

Nucleophilicity [29]

Domingo and his collaborators[28] proposed that molecules with low electrophilicity index are good nucleophiles. However, this hypothesis is only applicable to simple molecules. They demonstrated that complex molecules with multiple functional groups can be both good nucleophiles and good electrophiles.[30] Therefore, the nucleophilicity index cannot be defined as the inverse of the electrophilicity index.

Recently, Pérez et al. used the HOMO energies obtained by the Kohn-Sham method to describe the nucleophilicity index of molecules using the following equation:[31]

$$N = E_{HOMO_{Nu}} - E_{HOMO_{TCE}} \quad (8)$$

TCE, which stands for tetracyanoethylene, is used as a reference in this context.

In scientific literature, it is commonly observed that the nucleophilicity scale is calibrated with reference to the tetracyanoethylene (TCE) molecule. TCE is preferred as a reference molecule because it has the lowest HOMO energy amongst a wide range of molecules already investigated in the context of dipolar cycloadditions. The selection of TCE as a reference molecule facilitates the management of a nucleophilicity scale with positive values.

On the other hand, local reactivity indices describe the reactivity within each molecule. They provide reactivity information about specific regions, which consequently deduces areas that are more or less to undergo chemical reactions. The employed indices are quite similar to those used in the global reactivity indices, apart from the part where they are local, in other words, we use the calculated global indices to generate the local reactivity indices. In 2013, Domingo and al.[32,33] proposed Parr functions P^-, P^+.

$$P^-(r) = \rho_s^{rc}(r) \quad (9)$$

$$P^+(r) = \rho_s^{ra}(r) \quad (10)$$

where $\rho_s^{rc}(r)$is the atomic spin density of the radical cation, and $\rho_s^{ra}(r)$is the atomic spin density anion. Based on these equations, we can determine and calculate the local electrophilicity ω_k, and local nucleophilicity indices N_k.

$$N_k = NP_k^- \quad (11)$$

$$\omega_k = \omega P_k^+ \quad (12)$$

To locate the transition state of each product, single-point Berny optimization was conducted, and they were all confirmed by the frequency calculations, where only one imaginary frequency was detected, followed by IRC path generation. This latter confirms the reactants-TS-Products reaction path.

References

1. Huisgen, R. **(1963)** 1,3-Dipolar Cycloadditions. Past and Future. *Angew. Chem. Int. Ed. Engl. 2* (10), 565–598.
2. Singh, M. S.; Chowdhury, S.; Koley, S. **(2016)** Progress in 1,3-Dipolar Cycloadditions in the Recent Decade: An Update to Strategic Development towards the Arsenal of Organic Synthesis. *Tetrahedron*. *72* (13), 1603–1644.
3. Hashimoto, T.; Maruoka, K. **(2015)** Recent Advances of Catalytic Asymmetric 1,3-Dipolar Cycloadditions. *Chem. Rev. 115* (11), 5366–5412.
4. Wang, L.-J.; Tang, Y. **(2014)** Intermolecular 1,3-Dipolar Cycloadditions of Alkenes, Alkynes, and Allenes. In *Comprehensive Organic Synthesis II*. 4.22, 1342–1383.
5. Menon, R. S.; Nair, V. **(2014)** Intramolecular 1,3-Dipolar Cycloadditions of Alkenes, Alkynes, and Allenes. In *Comprehensive Organic Synthesis II*. 4.21, 1281–1341.
6. Yousfi, Y.; Benchouk, W.; Mekelleche, S. M. **(2023)** Prediction of the Regioselectivity of the Ruthenium-Catalyzed [3+2] Cycloadditions of Benzyl Azide with Internal Alkynes Using Conceptual DFT Indices of Reactivity. *Chem Heterocycl Comp*. *59* (3), 118–127.
7. Dresler, E.; Woliński, P.; Wróblewska, A.; Jasiński, R. **(2023**) On the Question of Zwitterionic Intermediates in the [3+2] Cycloaddition Reactions between Aryl Azides and Ethyl Propiolate. *Molecules. 28* (24), 8152.
8. Dresler, E.; Wróblewska, A.; Jasiński, R. **(2022)** Understanding the Regioselectivity and the Molecular Mechanism of [3 + 2] Cycloaddition Reactions between Nitrous Oxide and Conjugated Nitroalkenes: A DFT Computational Study. *Molecules*. *27* (23), 8441.
9. Zawadzińska, K.; Gadocha, Z.; Pabian, K.; Wróblewska, A.; Wielgus, E.; Jasiński, R. **(2022)** The First Examples of [3+2] Cycloadditions with the Participation of (E)-3,3,3-Tribromo-1-Nitroprop-1-Ene. *Materials*. *15* (21), 7584.
10. Umar, A. R.; Tia, R.; Adei, E. **(2021)** The 1,3-Dipolar Cycloaddition of Adamantine-Derived Nitrones with Maleimides: A Computational Study. *Computational and Theoretical Chemistry*. *1195*, 113099.
11. Jasiński, R. **(2015)** In the Searching for Zwitterionic Intermediates on Reaction Paths of [3 + 2] Cycloaddition Reactions between 2,2,4,4-Tetramethyl-3-Thiocyclobutanone S-Methylide and Polymerizable Olefins. *RSC Adv. 5* (122), 101045–101048.
12. Jasiński, R. **(2015)** A Stepwise, Zwitterionic Mechanism for the 1,3-Dipolar Cycloaddition between (Z)-C-4-Methoxyphenyl-N-Phenylnitrone and Gem-Chloronitroethene Catalysed by 1-Butyl-3-Methylimidazolium Ionic Liquid Cations. *Tetrahedron Letters*. *56* (3), 532–535.
13. Kaushik, C. P.; Pahwa, A.; Singh, D.; Kumar, K.; Luxmi, R. **(2019)** Efficient Synthesis, Antitubercular and Antimicrobial Evaluation of 1,4-Disubstituted 1,2,3-Triazoles with Amide Functionality. *Monatsh Chem*. *150* (6), 1127–1136.
14. Koubi Y., Hajji H., Moukhliss Y., El Khatabi K., El Masaoudy Y., Maghat H. Ajana M.A., Bouachrine M., Lakhlifi T. **(2022)** In Silico Studies of 1,4-Disubstituted 1,2,3-Triazole with Amide Functionality Antimicrobial Evaluation

against Escherichia Coli Using 3D-QSAR, Molecular Docking, and ADMET Properties. *Mor. J. Chem*. 10(4), 689-702.
15. Aurell, M. J.; Domingo, L. R.; Pérez, P.; Contreras, R. **(2004)** A Theoretical Study on the Regioselectivity of 1,3-Dipolar Cycloadditions Using DFT-Based Reactivity Indexes. *Tetrahedron*. *60* (50), 11503–11509.
16. García, J. I.; Martínez-Merino, V.; Mayoral, J. A.; Salvatella, L. **(1998)** Density Functional Theory Study of a Lewis Acid Catalyzed Diels−Alder Reaction. The Butadiene + Acrolein Paradigm. *J. Am. Chem. Soc. 120* (10), 2415–2420.
17. Birkholz, A. B.; Schlegel, H. B. **(2015)** Using Bonding to Guide Transition State Optimization. *J. Comput. Chem. 36* (15), 1157–1166.
18. Wiberg, K. B. **(1968)** Application of the Pople-Santry-Segal CNDO Method to the Cyclopropylcarbinyl and Cyclobutyl Cation and to Bicyclobutane. *Tetrahedron*. *24* (3), 1083–1096.
19. Lendvay, G. **(1994)** Characterization of the Progress of Chemical Reactions by Ab Initio Bond Orders. *J. Phys. Chem. 98* (24), 6098–6104.
20. Geerlings, P.; De Proft, F.; Langenaeker, W. **(2003)** Conceptual Density Functional Theory. *Chem. Rev. 103* (5), 1793–1874. https://doi.org/10.1021/cr990029p.
21. Domingo, L.; Ríos-Gutiérrez, M.; Pérez, P. **(2016)** Applications of the Conceptual Density Functional Theory Indices to Organic Chemistry Reactivity. *Molecules*. *21* (6), 748.
22. Becke, A. D. **(1993)** Density-functional Thermochemistry. III. The Role of Exact Exchange. *The Journal of Chemical Physics*. *98* (7), 5648–5652.
23. Lee, C.; Yang, W.; Parr, R. G. **(1988)** Development of the Colle-Salvetti Correlation-Energy Formula into a Functional of the Electron Density. *Phys. Rev. B*. *37* (2), 785–789.
24. Hehre, W. J., Ed. (**1993)** Ab Initio Molecular Orbital Theory, A Wiley-Interscience Publication; Wiley: New York.
25. Grimme, S.; Antony, J.; Ehrlich, S.; Krieg, H. **(2010)** A Consistent and Accurate *Ab Initio* Parametrization of Density Functional Dispersion Correction (DFT-D) for the 94 Elements H-Pu. *The Journal of Chemical Physics*. *132* (15), 154104.
26. Pearson, R. G. **(1988)** Absolute Electronegativity and Hardness: Application to Inorganic Chemistry. *Inorg. Chem. 27* (4), 734–740.
27. Domingo, L. R.; Aurell, M. J.; Pérez, P.; Contreras, R. **(2002)** Quantitative Characterization of the Global Electrophilicity Power of Common Diene/Dienophile Pairs in Diels–Alder Reactions. *Tetrahedron*. *58* (22), 4417–4423.
28. Parr, R. G.; Szentpály, L. v.; Liu, S. **(1999)** Electrophilicity Index. *J. Am. Chem. Soc. 121* (9), 1922–1924.
29. Domingo, L. R.; Pérez, P. **(2011)** The Nucleophilicity N Index in Organic Chemistry. *Org. Biomol. Chem. 9* (20), 7168.
30. Domingo, L. R.; Chamorro, E.; Pérez, P. **(2008)** Understanding the Reactivity of Captodative Ethylenes in Polar Cycloaddition Reactions. A Theoretical Study. *J. Org. Chem. 73* (12), 4615–4624.
31. Jaramillo, P.; Domingo, L. R.; Chamorro, E.; Pérez, P. **(2008)** A Further Exploration of a Nucleophilicity Index Based on the Gas-Phase Ionization Potentials. *Journal of Molecular Structure: THEOCHEM*. *865* (1–3), 68–72.
32. Domingo, L. R.; Pérez, P.; Sáez, J. A. **(2013)** Understanding the Local Reactivity in Polar Organic Reactions through Electrophilic and Nucleophilic Parr Functions. *RSC Adv. 3* (5), 1486–1494.
33. Chamorro, E.; Pérez, P.; Domingo, L. R. **(2013)** On the Nature of Parr Functions to Predict the Most Reactive Sites along Organic Polar Reactions. *Chemical Physics Letters*. *582*, 141–143.